Electronic Research Archive

https://www.aimspress.com/journal/era

ERA, 34(5): 3530–3553.
DOI: 10.3934/era.2026158
Received: 10 March 2026
Revised: 15 April 2026
Accepted: 16 April 2026
Published: 23 April 2026

Research article

Dynamic modeling and analysis for the periodic spread of influenza: A case study in Shanghai

Zhenwen Qin and Xichao Duan*

College of Science, University of Shanghai for Science and Technology, Shanghai 200093, China

* **Correspondence:** Email: xcduan@usst.edu.cn.

Abstract: In this paper, an $SIRS$ epidemic model with periodic transmission and vaccination is proposed to study the periodic transmission phenomenon of influenza. The threshold dynamics of the model are completely determined by the basic reproduction number $\mathcal{R}_0$, i.e., the disease-free periodic steady state is globally asymptotically stable if $\mathcal{R}_0 < 1$, while the disease is uniformly persistent if $\mathcal{R}_0 > 1$. With the help of control theory, the resonance frequency ω_r of our model is obtained, which is numerically validated in that there exists a resonance phenomenon of the disease spread (i.e., there is a maximum amplitude of the oscillatory spread of diseases) when the frequency $\omega = \omega_r$. By fitting the real data of influenza from Shanghai, we estimate the parameter values of the model. Results show that there is no resonance phenomenon in the spread of influenza in Shanghai. Based on the expression of resonance frequency ω_r, the effects of the mean transmission rate β and the transition rate δ on the resonance frequency ω_r are displayed numerically.

Keywords: influenza; $SIRS$ model; oscillation; uniform persistence; resonance frequency

1. Introduction

Influenza is an acute respiratory infectious disease caused by the influenza virus. Influenza A and B viruses of the *Orthomyxoviridae* family are the main pathogens of this acute viral respiratory disease (including four subtypes A(H_1N_1), A(H_3N_2), B/Yamagata, and B/Victoria). The influenza viruses are characterized by antigenic variability, strong infectivity, and rapid transmission, and they cause seasonal influenza epidemics every year [1, 2]. Besides the changes in contact frequency brought about by human seasonal behavioral patterns [3], the influenza epidemic seasonal activities are closely influenced by climatic factors [4]. Temperature and humidity always play key roles in the survival and transmissibility of the virus [5]. In temperate climate regions, influenza exhibits a distinct "flu season" pattern: A large-scale outbreak occurs every winter, while influenza activity disappears during warm seasons [6]. Especially, the influenza epidemic shows differences between the north and the south of

China, i.e., there is a single peak in winter in the north of China, while there is a double peak in winter and summer in the south of China [7].

Modeling and analysis for the seasonal transmission of influenza are challenging and complex, including statistical models [8, 9], differential equation models [10–18], epidemiological models based on pulse vaccination strategies [19, 20], non-autonomous periodic epidemic models [21–25], etc. To deeply reveal the periodic characteristics and internal mechanisms of influenza transmission, researchers often rely on dynamic theory for quantitative characterization and mechanism analysis. Based on the data of influenza and climate in Pudong New Area of Shanghai, Zhang et al. established some statistical models, including a generalized linear model, a distributed lag nonlinear model, and a regression tree model, to study the relationship between climate and transmission of influenza A and B. Results show that climate has a complex nonlinear relationship with the transmission of two types of influenza [8]. Besides that, many differential equation models are used to study the periodic transmission of influenza [13–15]. Combining a continuous differential equation with discrete inter-seasonal mappings, Asaduzzaman et al. proposed a hybrid epidemic model to study the phenomenon of strain replacement of influenza virus during the process of influenza transmission, and revealed the effects of vaccination on the periodic transmission of influenza [13]. Duan et al. proposed an age-structured $SIRS$ model with age of recovery to study the roles of age of recovery on the existence of global Hopf bifurcation, and then revealed the cause of the periodic transmission of disease [16]. Periodic transmission of influenza can also be modeled by using a pulse epidemic model [19].

Nonautonomous epidemic models are used to study the transmission of influenza [21–24]. For example, Teng et al. established a class of non-autonomous $SIRS$ epidemic models with a periodic transmission rate and a disease-induced mortality to study the transmission and control of the disease. By analysis, they obtained the necessary and sufficient conditions for disease persistence and extinction [21]. Besides the periodic transmission rate, periodic vaccination also plays an important role on the spread of influenza. Moneim established an $SIRS$ epidemic model with periodic vaccination to study the transmission and control of H_1N_1 influenza [25]. The periodic dynamic behaviors of the $SIRS$ epidemic model are determined by the basic reproduction number $\mathcal{R}_0$, which shows that seasonal immunization strategies are more useful in the control of influenza. Kumar et al. proposed autonomous and nonautonomous $SIRS$ epidemic models to study the dynamics of the transmission of influenza. By comparison, results show that seasonal forces (periodic transmission rate and periodic recover rate) can give rise to periodic oscillations, quasi-periodicity, and even chaotic behaviors [23]. In 2004, based on the real data of the transmission of influenza, Dushoff et al. proposed an $SIRS$ epidemic model with periodic transmission rate to study the oscillation of the transmission of influenza. They revealed a resonance mechanism of the seasonal influenza transmission which shows that slight changes can lead to strong oscillations in the spread of the disease [26]. Theoretically, there is a frequency ω_r that is expressed by other parameters of the epidemic model, such that the amplitude of the solution reaches its maximum value when the frequency $\omega = \omega_r$, then we call ω_r the resonance frequency of the epidemic model. For more information about resonance frequency, one can refer to [27].

Motivated by the above discussions, we will collect the data of influenza from Shanghai and model the spread of influenza in Shanghai by an $SIRS$ epidemic model with a periodic transmission rate and a periodic vaccination rate. Note that there are two input frequencies from transmission and vaccination in our model. Data fitting and theoretical analysis of the model will bring us many challenges. Whether

there is a resonant phenomenon in our model and how disease transmission parameters affect the resonant frequency are our primary concerns.

The structure of this study is organized as follows. In Section 2, statistical analysis of the monthly infection data of influenza in Shanghai from June 2014 to May 2016 is carried out to capture the seasonal pattern, and then an $SIRS$ epidemic model with periodic transmission and vaccination is formulated. In Section 3, the dynamic behaviors of our $SIRS$ epidemic model are strictly proved. The main results, i.e., the existence of the resonance phenomena of our model, are presented and strictly proved with help of resonance theory. In Section 4, some numerical simulations are carried out to illustrate the resonance phenomena of our model. By use of real data from Shanghai, the parameters of our model are well-fitted. After that, the influence of different parameter values on the resonance frequency is verified by numerical examples. Finally, a brief conclusion and discussion are presented in Section 5.

2. Modeling

2.1. Data analysis

The data of new cases of influenza in the months from June 2014 to April 2016 of Shanghai are selected as the subject, taken from the Shanghai Municipal Health Commission [28]. As shown in the bar chart of Figure 1, the disease transmission has a distinct periodicity and fluctuates in a cyclical pattern with two peaks within a year. The number of cases in winter and summer are significantly higher than that in spring and autumn. Seasonality is a notable characteristic of the spread of influenza. These data can be fitted by trigonometric functions numerically, which has a specific expression,

$$X_t = (3.385 + 2.935\sin(\omega t) - 1.369\cos(\omega t)) \times 10^{-7} \text{ with } \omega = \frac{2\pi}{11.66}.$$

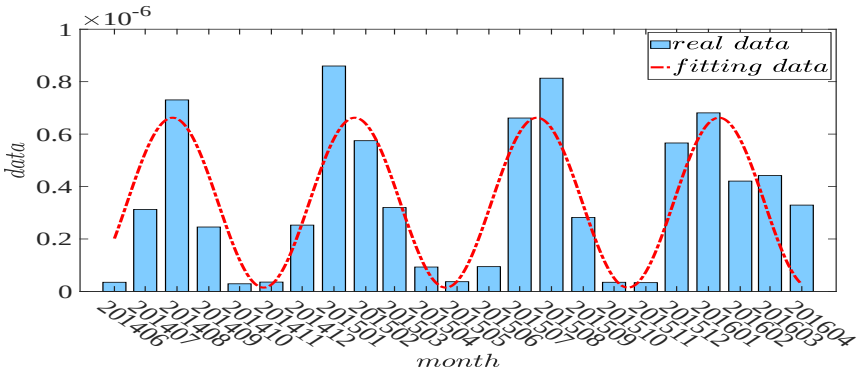

Figure 1. Monthly data on human influenza cases in Shanghai.

Note that there are two characteristics of influenza data from Shanghai, including seasonal transmission and variation of the illness. Consequently, it is necessary to implement vaccination strategies periodically. Thus, we need to formulate an epidemic model involving periodic transmission rate with a frequency ω_1 and periodic vaccination rate with a frequency ω_2 to model the transmission of the Shanghai influenza. To get a better theoretical analysis, mathematically, we should adopt the greatest common factor of ω_1 and ω_2 as the frequency of transmission and vaccination in the epidemic modeling.

In a periodic dynamical model, besides the dynamic results including the global stability of the disease-free steady state and the uniform persistence of the disease, there is often a resonance phenomenon induced by a resonant frequency. Whether resonance phenomena will occur in the dynamics of our epidemic model and whether resonance phenomena will occur in the future spread of diseases with environmental changes and virus mutations are both key concerns. To address this point, we will apply the methods and feedback control theory proposed in [27].

2.2. Model formulation

The periodic dynamics of influenza epidemics can be described by using a standard $SIRS$ model, driven by periodic variations in susceptibility and vaccination. $S(t)$ is the number of susceptible individuals at time t, $I(t)$ is the number of infectious individuals at time t, $R(t)$ is the number of recovered individuals at time t, and $N(t)$ is the total number of the population at time t. The disease infection coefficient $\beta(t)$ consists of two parts: the mean transmission rate β and the periodic fluctuation of susceptibility $\beta\Delta\beta\sin\omega t$, driven by the environment. The vaccination rate $\eta(t)$ also consists of two parts: the mean vaccination rate η and the periodic fluctuation of vaccination $\eta\Delta\eta\sin\omega t$. It is assumed that these two fluctuation frequencies are equal. Then, the model takes the form of

$$\begin{cases} \dfrac{dS(t)}{dt} = \mu N(t) - (\mu + \eta(t))S(t) - \beta(t)\dfrac{I(t)}{N(t)}S(t) + \delta R(t), \\ \dfrac{dI(t)}{dt} = \beta(t)\dfrac{I(t)}{N(t)}S(t) - (\mu + \nu)I(t), \\ \dfrac{dR(t)}{dt} = \eta(t)S(t) + \nu I(t) - (\mu + \delta)R(t), \\ S(0) = S_0,\ I(0) = I_0,\ R(0) = R_0, \end{cases} \tag{2.1}$$

where $\beta(t) = (1 + \Delta\beta\sin\omega t)\beta$, $\eta(t) = (1 + \Delta\eta\sin\omega t)\eta$. The parameter μ is the natural birth rate and death rate of the population, ν is the recovery rate of infected individuals, and δ is the transition rate from the recovered to the susceptible. Note that $N(t) = S(t) + I(t) + R(t)$. We have $\frac{dN(t)}{dt} = 0$; then, the total number of the population is a constant $N(t) \equiv N$.

Let $x(t) = \frac{S(t)}{N}$, $y(t) = \frac{I(t)}{N}$, and $z(t) = \frac{R(t)}{N}$. Model (2.1) can be rewritten as

$$\begin{cases} \dfrac{dx(t)}{dt} = \mu - \mu x(t) - \eta(t)x(t) - \beta(t)x(t)y(t) + \delta z(t), \\ \dfrac{dy(t)}{dt} = \beta(t)x(t)y(t) - (\mu + \nu)y(t), \\ \dfrac{dz(t)}{dt} = \eta(t)x(t) + \nu y(t) - (\mu + \delta)z(t), \\ x(0) = x_0,\ y(0) = y_0,\ z(0) = z_0. \end{cases} \tag{2.2}$$

Substituting $z = 1 - x - y$ into the first equation of model (2.2), we obtain

$$\begin{cases} \dfrac{dx(t)}{dt} = (\mu + \delta) - (\mu + \delta + \eta(t))x(t) - \beta(t)x(t)y(t) - \delta y(t), \\ \dfrac{dy(t)}{dt} = \beta(t)x(t)y(t) - (\mu + \nu)y(t), \\ x(0) = x_0,\ y(0) = y_0. \end{cases} \tag{2.3}$$

In the following, we will mainly study the dynamics of model (2.3).

3. Dynamics analysis

In order to understand the impact of periodic vaccination and periodic transmission on the spread of disease described by model (2.3), we first studied the stability of the positive equilibrium of model (2.3) under constant vaccination and constant transmission, i.e., $\Delta\beta = 0$ and $\Delta\eta = 0$.

3.1. Stability of the positive equilibrium of model (2.3) *when* $\Delta\beta = 0$ *and* $\Delta\eta = 0$.

To study model (2.3), we first make the following simplifications: $\Delta\beta = 0$ and $\Delta\eta = 0$. Then, model (2.3) can be transformed into

$$\begin{cases} \dfrac{dx(t)}{dt} = (\mu + \delta) - (\mu + \eta + \delta)x(t) - \beta x(t)y(t) - \delta y(t), \\ \dfrac{dy(t)}{dt} = \beta x(t)y(t) - (\mu + \nu)y(t). \end{cases} \tag{3.1}$$

According to the definition of the basic reproduction number, we define the basic reproduction number of model (3.1) as

$$\mathcal{R}_{01} = \frac{(\mu + \delta)\beta}{(\mu + \nu)(\mu + \eta + \delta)}.$$

Theorem 3.1. *If* $\mathcal{R}_{01} > 1$, *model* (3.1) *has a unique positive equilibrium* $E^* = (x^*, y^*)$, *which is locally stable, where*

$$x^* = \frac{\mu + \nu}{\beta}, \quad y^* = \frac{\mu + \delta}{\mu + \nu + \delta} - \frac{(\mu + \eta + \delta)(\mu + \nu)}{\beta(\mu + \nu + \delta)}. \tag{3.2}$$

Proof. From the two equations of model (3.1), we have the positive equilibrium, which satisfies the following equations:

$$\begin{cases} 0 = (\mu + \delta) - (\mu + \eta + \delta)x^* - \beta x^* y^* - \delta y^*, \\ 0 = \beta x^* y^* - (\mu + \nu)y^*. \end{cases}$$

It follows that

$$x^* = \frac{\mu + \nu}{\beta}$$

and

$$y^* = \frac{\mu + \delta}{\mu + \nu + \delta} - \frac{(\mu + \eta + \delta)(\mu + \nu)}{\beta(\mu + \nu + \delta)} = \frac{1}{\beta(\mu + \nu + \delta)}(\mathcal{R}_{01} - 1) > 0,$$

if $\mathcal{R}_{01} > 1$.

Linearizing model (3.1) at the positive equilibrium (x^*, y^*), we have the following characteristic equation:

$$\begin{vmatrix} \lambda + \mu + \delta + \eta + \beta y^* & \beta x^* + \delta \\ -\beta y^* & \lambda - \beta x^* + \mu + \nu \end{vmatrix} = \lambda^2 + b_{01}\lambda + b_{02} = 0, \tag{3.3}$$

with $b_{01} = (\mu + \delta + \eta) + \beta y^* > 0$, $b_{02} = \beta^2 x^* y^* + \delta\beta y^* > 0$. Thus, the positive equilibrium (x^*, y^*) of model (3.1) is locally stable if $\mathcal{R}_{01} > 1$.

3.2. Extinction and uniform persistence of disease

Obviously, model (2.3) has a disease-free periodic equilibrium $E^0 = (x^0(t), 0)$, which satisfies

$$\begin{cases} \dfrac{dx}{dt} = \mu + \delta - (\mu + \delta + \eta(t))x(t), \\ x(0) = x_0. \end{cases} \tag{3.4}$$

Clearly, solving (3.4), we have

$$x^0(t) = e^{-\int_0^t (\mu+\delta+\eta(\tau))d\tau}\left(x_0 + (\mu+\delta)\int_0^t e^{\int_0^s (\mu+\delta+\eta(\tau))d\tau} ds\right).$$

To get the stability of the disease-free periodic equilibrium $E^0 = (x^0(t), 0)$, we will use the method in [29, 30]. Following from the second equation of model (2.3), we define $\mathcal{F}(t) = \beta(t)Nx^0(t)$ and $\mathcal{V} = \mu + \nu$. Assume $\mathcal{Y}(t, s)$ $(t \geq s)$ is the evolution operator of $\frac{dy(t)}{dt} = -\mathcal{V}y(t)$. Thus, for $\forall s \in \mathbb{R}$, the operator $\mathcal{Y}(t, s)$ satisfies

$$\frac{d\mathcal{Y}(t, s)}{dt} = -\mathcal{V}\mathcal{Y}(t, s), \quad \forall t \geq s,\ \mathcal{Y}(s, s) = \mathbb{I}.$$

Let C_T denote the Banach space of a T-periodic function from $\mathbb{R}$ to $\mathbb{R}$. If $\phi \in C_T$ is the initial distribution of infectious individuals, then $\mathcal{F}(s)\phi(s)$ represents the rate at which infected individuals generate new infections at time s, and $\mathcal{Y}(t, s)\mathcal{F}(s)\phi(s)$ with $t \geq s$ gives the distribution of infected individuals who are newly infected at time s and still remain in state y at time t [30]. By the approaches used in [29, 30], we can define the generation operator $\mathcal{L}$: $C_T \to C_T$ as

$$\mathcal{L}(\phi(t)) = \int_0^\infty \mathcal{Y}(t, t-a)\mathcal{F}(t-a)\phi(t-a)da, \quad (\forall t \in \mathbb{R},\ \phi \in C_T).$$

$\mathcal{L}(\phi(t))$ is the distribution of newly infected individuals accumulated at time t. The basic reproduction number is defined as the spectral radius of the next generation operator $\mathcal{L}$, that is

$$\mathcal{R}_0 := \rho(\mathcal{L}),$$

where ρ denotes the spectral radius of the operator $\mathcal{L}$.

Theorem 3.2. *If $\mathcal{R}_0 < 1$, the disease-free periodic equilibrium E^0 of model* (2.3) *is globally asymptotically stable.*

Proof. See Appendix A.

For more information about the uniform persistence of an periodic epidemic model, one can refer to references [31, 32]. In the following, we set

$$H_0 = \left\{(x, y) \in \mathbb{R}^2_+ : y > 0\right\},\ \partial H_0 = \mathbb{R}^2_+ \setminus H_0.$$

Theorem 3.3. *If $\mathcal{R}_0 > 1$, the disease described by model* (2.3) *is uniformly persistence with respect to H_0, i.e., there exists $\varepsilon > 0$ such that any solution of model* (2.3) *with the initial conditions in H_0 satisfies $\liminf_{t\to\infty} y(t) > \varepsilon$.*

Proof. See Appendix B.

3.3. Resonance phenomena

In the case when $\Delta\eta = \Delta\beta = 0$ or $\omega = 0$, model (2.3) has a positive equilibrium (x^*, y^*), and it is locally stable if $\mathcal{R}_{01} > 1$, as follows from Theorem 3.1. There is a damped oscillation of the system without periodic input control. In the case where, $\Delta\eta \neq 0$, $\Delta\beta \neq 0$, and $\omega \neq 0$, there will be periodic dynamic behaviors of model (2.3), as follows from Theorems 3.2 and 3.3. There is a continuous oscillation phenomenon of the system with periodic terms. To further study the effect of the frequency ω on the periodic dynamic behavior of model (2.3), we will apply the control theory in our epidemic model and present a definition of *resonance frequency* [27].

Definition 3.1. *Assume that $y(t) = g(\omega)\sin(\omega t + \phi)$ is a solution of model* (2.3)*. We say there is a resonance frequency ω_r of $y(t)$ if the amplitude of $y(t)$ has a maximum point ω_r, i.e., $g(\omega)$ reaches its maximum value when $\omega = \omega_r$.*

From Definition 3.1, we say there is a resonance phenomenon of the periodic epidemic model when the input frequency equals the resonance frequency. To prove there is a resonance phenomenon of (2.3) when the dynamic behavior of model (2.3) reaches a steady state, we define

$$x(t) = x_1(t) + x^*, \quad y(t) = y_1(t) + y^*,$$

where x_1 and y_1 represent the variations in x and y at the positive equilibrium (x^*, y^*) of model (3.1). Substituting $x(t)$ and $y(t)$ into model (2.3), we obtain

$$\begin{cases} \dfrac{dx_1}{dt} = -(\mu + \eta + \delta + \beta y^*)x_1(t) - (\mu + \nu + \delta)y_1(t) \\ \qquad - \eta x^* \Delta\eta \sin(\omega t) - (\mu + \nu)y^* \Delta\beta \sin(\omega t), \\ \dfrac{dy_1}{dt} = (\mu + \nu)y^* \Delta\beta \sin(\omega t) + \beta y^* x_1(t). \end{cases} \tag{3.5}$$

By taking the derivative of both sides of the first equation of (3.5), with respect to time t simultaneously, and using the second equation of (3.5), we obtain

$$x_1'' + (\mu + \eta + \delta + \beta y^*)x_1' + (\mu + \nu + \delta)\beta y^* x_1 = u(t), \tag{3.6}$$

where $u(t) = -r_1 \sin(\omega t) - r_2 \omega \cos(\omega t)$ with

$$r_1 = (\mu + \nu)(\mu + \nu + \delta)y^* \Delta\beta, \quad r_2 = \eta \Delta\eta x^* + (\mu + \nu)y^* \Delta\beta.$$

Obviously, the input term $u(t) = 0$ if $\Delta\beta = \Delta\eta = 0$ or $\omega = 0$.

From the standard form of the second-order linear dynamic system, we can transfer (3.6) into the following second-order linear dynamic system:

$$x_1'' + 2\omega_n \zeta x_1' + \omega_n^2 x_1 = u(t) = -r_1 \sin(\omega t) - r_2 \omega \cos(\omega t) \tag{3.7}$$

with

$$\omega_n = \sqrt{(\mu + \nu + \delta)\beta y^*}, \quad \zeta = \frac{\mu + \eta + \delta + \beta y^*}{2\sqrt{(\mu + \delta + \nu)\beta y^*}}.$$

Here, ω_n is called the undamped natural frequency, and ζ is the damping ratio of the solutions of the dynamic model (3.7) (see [27]). For simplicity, we assume that $0 < \zeta < \frac{\sqrt{2}}{2}$.

The main result of our model (2.3) can be presented as the following Theorems 3.4 and 3.5.

Theorem 3.4. *If $\mathcal{R}_{01} > 1$, the amplitude of $y_1(t)$ of model* (3.5) *has a maximum point ω_r, i.e., a resonance phenomenon of the $y(t)$ of model* (2.3) *occurs when $\omega = \omega_r$.*

Proof. Clearly, the dynamic model (3.7) can be solved:

$$x_1(t) = \hat{x}_1(t) + \tilde{x}_1(t), \tag{3.8}$$

where $\tilde{x}_1(t)$ is a special solution of (3.7), and $\hat{x}_1(t)$ is the general solution the following homogeneous equation

$$x_1^{''} + 2\omega_n\zeta x_1^{'} + \omega_n^2 x_1 = 0. \tag{3.9}$$

By some direct calculations, we have

$$\hat{x}_1(t) = e^{-\sigma t}(c_1\cos(\omega_d t) + c_2\sin(\omega_d t)), \;\; 0 < \zeta < 1, \tag{3.10}$$

with some undetermined real numbers c_1, c_2, and $\sigma = -\zeta\omega_n$, $\omega_d = \omega_n\sqrt{(1-\zeta^2)}$, which is called as the damped natural frequency [27]. The special solution $\tilde{x}_1(t)$ of (3.7) can be obtained by use of the undetermined coefficient method:

$$\tilde{x}_1(t) = A_1(\omega)\cos(\omega t) + A_2(\omega)\sin(\omega t) \tag{3.11}$$

with

$$A_1(\omega) = \frac{-r_2\omega(\omega_n^2-\omega^2) + 2r_1\zeta\omega_n\omega}{(2\zeta\omega_n\omega)^2 + (\omega_n^2-\omega^2)^2}, \; A_2(\omega) = \frac{-r_1(\omega_n^2-\omega^2) - 2r_2\zeta\omega_n\omega^2}{(2\zeta\omega_n\omega)^2 + (\omega_n^2-\omega^2)^2}. \tag{3.12}$$

The solution $\tilde{x}_1(t)$ in (3.11) can be transferred as the following form:

$$\tilde{x}_1(t) = \sqrt{A_1^2(\omega) + A_2^2(\omega)}\cos(\omega t + \phi), \tag{3.13}$$

with $\phi = \arctan\frac{-A_2(\omega)}{A_1(\omega)}$ and

$$\sin\phi = \frac{-A_2(\omega)}{\sqrt{A_1^2(\omega) + A_2^2(\omega)}}, \; \cos\phi = \frac{A_1(\omega)}{\sqrt{A_1^2(\omega) + A_2^2(\omega)}}. \tag{3.14}$$

To determine the undetermined real numbers c_1 and c_2 in (3.10), we need the initial conditions $x_1(0) = x_{10}$ and $y_1(0) = y_{10}$. From (3.8), (3.10) and (3.11), we have $x_{10} = x_1(0) = c_1 + A_1(\omega)$. Then,

$$c_1 = x_{10} - A_1(\omega). \tag{3.15}$$

From the first equation of (3.5), we have

$$\left.\frac{dx_1}{dt}\right|_{t=0} = -(\mu + \eta + \delta + \beta y^*)x_{10} - (\mu + \nu + \delta)y_{10}.$$

Meanwhile, from (3.8), (3.10), and (3.11), we have

$$\left.\frac{dx_1}{dt}\right|_{t=0} = \left.\frac{d\hat{x}_1}{dt}\right|_{t=0} + \left.\frac{d\tilde{x}_1}{dt}\right|_{t=0} = -\sigma c_1 + \omega_d c_2 + \omega A_2(\omega).$$

Thus, we have

$$\begin{aligned} c_2 &= \frac{1}{\omega_d}\left(\sigma c_1 - \omega A_2(\omega) - (\mu+\eta+\delta+\beta y^*)x_{10} - (\mu+\nu+\delta)y_{10}\right) \\ &= \frac{1}{\omega_d}\left(\sigma(x_{10}-A_1(\omega)) - 2\omega_n\zeta x_{10} - h y_{10} - \omega A_2(\omega)\right). \end{aligned} \tag{3.16}$$

Substituting the general solution (3.8) into the second equation of (3.5), we have

$$\frac{dy_1}{dt} = \frac{r_1}{h}\sin(wt) + \frac{\omega_n^2}{h}\tilde{x}_1(t) + \frac{\omega_n^2}{h}\hat{x}_1(t), \tag{3.17}$$

with $h = \mu + \nu + \delta$. It follows from (3.13), (3.14), and (3.17) that

$$\frac{dy_1}{dt} = \frac{1}{h}\left(\omega^2 g(\omega)\right)^{\frac{1}{2}}\cos(\omega t + \psi) + \frac{\omega_n^2}{h}\hat{x}_1(t), \tag{3.18}$$

with

$$g(\omega) = \frac{\omega_n^4(A_1^2(\omega) + A_2^2(\omega)) + r_1^2 + 2r_1\omega_n^2 A_2(\omega)}{\omega^2}, \tag{3.19}$$

and

$$\psi = \arctan\frac{-A_2(\omega)\omega_n^2 - r_1}{A_1(\omega)\omega_n^2}.$$

Integrating both sides of Eq (3.18) simultaneously on the interval $[0, t]$, we obtain

$$y_1(t) = \hat{y}_1(t) + \frac{\omega_n^2}{h}\int_0^t \hat{x}_1(\tau)d\tau \tag{3.20}$$

with

$$\hat{y}_1(t) = y_{10} + \frac{g^{\frac{1}{2}}(\omega)}{h}\left(\sin(\omega t + \psi) - \sin(\psi)\right). \tag{3.21}$$

Obviously, $\hat{y}_1(t)$ is a periodic function of time t. It follows from (3.10) that

$$\frac{\omega_n^2}{h}\int_0^\infty \hat{x}_1(\tau)d\tau = \text{a constant } C$$

for $\zeta > 0$. It follows from (3.20) that there exists a large time T such that

$$y_1(t) \approx \hat{y}_1(t) + C \text{ for } t > T.$$

Clearly, the amplitude of $y_1(t)$ approximately equals that of $\hat{y}_1(t)$, which is determined by the function $g(\omega)$ in (3.19).

In order to find the maximum point ω_r of the function $g(\omega)$, we will use the extreme value theorem. Let $s = \omega^2$. It follows from (3.12) and (3.19) that we can transfer the function $g(\omega)$ to $f(s)$, i.e.,

$$g(\omega) = \frac{r_1^2 s + r_2^2\omega_n^4 + 4r_1^2\omega_n^2\zeta^2 - 4r_1 r_2\omega_n^3\zeta}{s^2 + \omega_n^4 + (4w_n^2\zeta^2 - 2\omega_n^2)s} := f(s). \tag{3.22}$$

Obviously, when $\zeta \in (0,1)$, the denominator of (3.22) is always greater than 0 on $s \in (0,+\infty)$. Differentiating the function $f(s)$ with respect to s, we have

$$f^{'}(s) = \frac{a_1 s^2 + a_2 s + a_3}{\left(s^2 + \omega_n^4 + (4\omega_n^2\zeta^2 - 2\omega_n^2)s\right)^2},$$

where

$$\begin{cases} a_1 = -r_1^2 < 0, \\ a_2 = -2\omega_n^2 (r_2\omega_n - 2\zeta r_1)^2 < 0, \\ a_3 = \left(2(1-2\zeta^2)(r_2\omega_n - 2r_1\zeta)^2 + r_1^2\right)\omega_n^4. \end{cases} \tag{3.23}$$

Clearly, the roots of $f'(s) = 0$ are determined by the numerator of $f'(s)$, which is denoted as $f_r(s) = a_1 s^2 + a_2 s + a_3$. Note that $a_1 < 0$ and $a_2 < 0$. If $0 < \zeta < \frac{\sqrt{2}}{2}$, we have $a_3 > 0$, and $f_r(s) = 0$ has a unique positive root $s_r = \frac{-a_2 + \sqrt{a_2^2 - 4a_1a_3}}{2a_1}$. Then, from Definition 3.1, the resonant frequency ω_r of $y_1(t)$ of model (3.5) can be obtained:

$$\omega_r = \sqrt{s_r} = \sqrt{\frac{-a_2 + \sqrt{a_2^2 - 4a_1a_3}}{2a_1}}. \tag{3.24}$$

Therefore, there is a resonance phenomenon of the solution $y_1(t)$ of model (3.5) when $\omega = \omega_r$, i.e., there is a resonance phenomenon of $y(t)$ of (2.3) that occurs when $\omega = \omega_r$.

Theorem 3.5. *If $\mathcal{R}_{01} > 1$, the amplitude of $x_1(t)$ of model* (3.5) *has a maximum point ω_{xr}, i.e., a resonance phenomenon of $x(t)$ of* (2.3) *occurs when $\omega = \omega_{xr}$.*

Proof. To prove there is a resonance phenomenon of $x(t)$ of (2.3), we need only to study the resonance frequency of $x_1(t)$ of model (3.5). Note that $x_1(t) = \hat{x}_1(t) + \tilde{x}_1(t)$. It follows from (3.10) that

$$\lim_{t\to\infty} \hat{x}_1(t) = \text{a constant } C_0 \text{ for } \zeta > 0.$$

Then, the amplitude of $x_1(t)$ approximately equals that of $\tilde{x}_1(t)$. From (3.13), the amplitude of $\tilde{x}_1(t)$ is determined by

$$\sqrt{A_1^2(\omega) + A_2^2(\omega)} = \sqrt{z(\omega)},$$

where

$$z(\omega) = \frac{r_1^2 + r_2^2\omega^2}{\omega^4 + \omega_n^4 + (4\omega_n^2\zeta^2 - 2\omega_n^2)\omega^2}. \tag{3.25}$$

If the function $z(\omega)$ has a maximum value at ω_{xr}, the amplitude of $x_1(t)$ will reach its maximum value at ω_{xr}. Similarly to the proof of Theorem 3.4, letting $s = \omega^2$, we can transfer the function $z(\omega)$ as a function $k(s)$:

$$z(\omega) = \frac{r_1^2 + r_2^2 s}{s^2 + \omega_n^4 + (4\omega_n^2\zeta^2 - 2\omega_n^2)s} := k(s). \tag{3.26}$$

Differentiating the function $k(s)$ with respect to s, we have

$$k'(s) = \frac{b_1 s^2 + b_2 s + b_3}{(s^2 + \omega_n^4 + (4\omega_n^2\zeta^2 - 2\omega_n^2)s)^2},$$

where

$$b_1 = -r_2^2 < 0, \;\; b_2 = -2r_1^2 < 0, \;\; b_3 = r_2^2\omega_n^4 + 2\omega_n^2 r_1^2(1 - 2\zeta^2). \tag{3.27}$$

Obviously, the roots of $k'(s) = 0$ are determined by the numerator of $k'(s)$, which is denoted as $k_r(s)$.

If $0 < \zeta < \frac{\sqrt{2}}{2}$, we have $b_3 > 0$. Note that $b_1 < 0$, $b_2 < 0$, and $\Delta_r = b_2^2 - 4b_1b_3$. It follows that there is a unique positive root s_{xr} of equation $k_r(s) = 0$, i.e., $s_{xr} = \frac{-2r_1^2 + \sqrt{\Delta_r}}{2r_2^2}$ if $b_3 > 0$. Then, from Definition 3.1, the resonant frequency ω_{xr} of the solution $x_1(t)$ in (3.8) can be obtained:

$$\omega_{xr} = \sqrt{s_{xr}} = \sqrt{\frac{-2r_1^2 + \sqrt{\Delta_r}}{2r_2^2}}. \tag{3.28}$$

Therefore, there is a resonance phenomenon of the solution $x_1(t)$ of model (3.5) when $\omega = \omega_{xr}$, i.e., there is a resonance phenomenon of $x(t)$ of (2.3) that occurs when $\omega = \omega_{xr}$.

In fact, the resonance phenomenon of the density of infection $y(t)$ of (2.3) is our main concerned. This phenomenon can help us to get a better understanding of the shortage of medical resources induced by a sharp increase in new infection cases.

4. Numerical analysis

4.1. Numerical simulation

In this subsection, some numerical simulations will be carried out to illustrate the results of Theorems 3.4 and 3.5, i.e., there are resonance phenomena of $y(t)$ and $x(t)$ of model (2.3) when $\omega = \omega_r$ and $\omega = \omega_{xr}$ respectively. We use months as the time unit. The parameter values are shown as follows.

$$\begin{cases} \mu = 0.005965, \; \nu = 6.72, \; \delta = 1.885470378731 \times 10^{-3}, \\ \beta = 9.629879, \; \Delta\beta = 7.06921 \times 10^{-10}, \\ \eta = 0.00235, \; \Delta\eta = 1.1831156005568 \times 10^{-2}. \end{cases} \tag{4.1}$$

By use of (4.1) and some calculations, we obtain $\mathcal{R}_{01} = 1.101898793165164$. It follows from (3.24) and (3.28) that

$$\omega_r = 0.083234060605095 \tag{4.2}$$

and

$$\omega_{xr} = 0.0883612637139263.$$

By use of (4.1), (3.19), and (3.25), we can plot the functions $g(\omega)$ and $z(\omega)$ in Figure 2. Numerical results show that there is a unique maximum point ω_r of the function $g(\omega)$ and a unique maximum point ω_{xr} of the function $z(\omega)$.

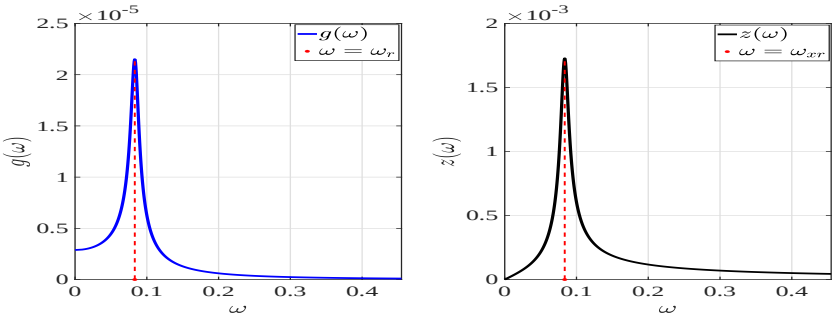

Figure 2. The graphs of the amplitude function $g(\omega)$ of (3.19) and the amplitude function $z(\omega)$ of (3.25).

To illustrate the role of the resonance frequency ω_r, we need the expression of $y_1(t)$ with initial conditions (x_{10}, y_{10}). From the expression of $\hat{x}_1(t)$, we obtain

$$\begin{aligned}\int_0^t \hat{x}_1(\tau)d\tau =& \int_0^t e^{-\sigma\tau}(c_1\cos(\omega_d\tau) + c_2\sin(\omega_d\tau))d\tau\\ =& c_1\int_0^t e^{-\sigma\tau}\cos(\omega_d\tau)d\tau + c_2\int_0^t e^{-\sigma\tau}\sin(\omega_d\tau)d\tau\\ =& y_{11}(t) + y_{12}(t),\end{aligned}$$

with

$$\begin{cases} y_{11}(t) = \dfrac{c_1}{(\sigma^2+\omega_d^2)}\left[(-\sigma\cos(\omega_d t) + \omega_d\sin(\omega_d t))e^{-\sigma t} + \sigma\right],\\ y_{12}(t) = \dfrac{c_2}{(\sigma^2+\omega_d^2)}\left[(-\sigma\sin(\omega_d t) - \omega_d\cos(\omega_d t))e^{-\sigma t} + \omega_d\right], \end{cases} \tag{4.3}$$

where the expressions of c_1 and c_2 are given by (3.15) and (3.16), respectively. It follows from (3.20) and (3.21) that

$$y_1(t) = \hat{y}_1(t) + \frac{\omega_n^2}{h}(y_{11}(t) + y_{12}(t)). \tag{4.4}$$

Substituting (3.15) and (3.16) into (4.4) and simplifying, we obtain the following equation,

$$y_1(t) = y_{01}(t) + y_{02}(t) + y_{03}(t),$$

where

$$\begin{aligned} y_{01}(t) = \frac{\omega_n^2}{h(\omega_d^2+\sigma^2)}\Bigg\{ & x_{10}\Bigg[e^{-\sigma t}\Big(\cos(\omega_d t)(-2\sigma - 2\omega_n\zeta) + \sin(\omega_d t)(\omega_d - \frac{\sigma}{\omega_d}(\sigma - 2\omega_n\zeta))\Big)\\ & + 2\sigma - 2\omega_n\zeta\Bigg] + y_{10}\Bigg[1 - \frac{h}{\omega_d}\left(e^{-\sigma t}\left(-\sigma\sin(\omega_d t) - \omega_d\cos(\omega_d t)\right) + \omega_d\right)\Bigg]\Bigg\}, \end{aligned}$$

$$\begin{aligned} y_{02}(t) = \frac{\omega_n^2}{h(\omega_d^2+\sigma^2)}\Bigg\{ & e^{-\sigma t}\Big(\cos(\omega_d t)[2\sigma A_1(\omega) + \omega A_2(\omega)]\\ & + \sin(\omega_d t)\Big[-\omega_d A_1(\omega) + \frac{\sigma^2 A_1(\omega) + \sigma\omega A_2(\omega)}{\omega_d}\Big]\Big) - 2\sigma A_1(\omega) - \omega A_2(\omega)\Bigg\}, \end{aligned}$$

and

$$y_{03}(t) = \frac{g^{\frac{1}{2}}(\omega)}{h}\left(\sin(\omega t + \psi) - \sin(\psi)\right).$$

$y_{01}(t)$ denotes the initial vibration component, $y_{02}(t)$ denotes the free vibration component, and $y_{01}(t)$ denotes the forced vibration component.

Assume that $x_{10} = 1.35 \times 10^{-8}$, and $y_{10} = 1.35 \times 10^{-8}$. The initial values of model (2.3) are assumed $x(0) = x^* + x_{10},\ y(0) = y^* + y_{10}$, and all parameters are shown in (4.1). From (3.24), we calculate the resonance frequency $\omega_r = 0.083234060605095$. From Theorem 3.4, there is a resonance phenomenon of the solution $y(t)$ of model (2.3) when $\omega = \omega_r$ (see Figure 3).

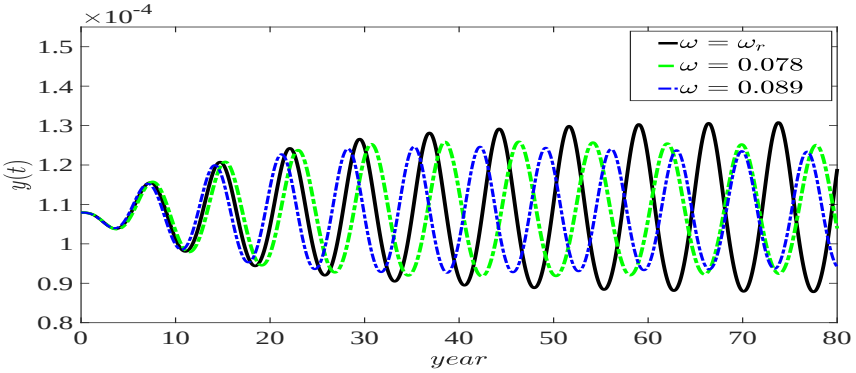

Figure 3. The solutions $y(t)$ of model (2.3) with $\omega = 0.078$, ω_r, and 0.89.

Note that all parameters are shown in (4.1). From (3.28), we calculate the resonance frequency $\omega_{xr} = 0.0883612637139263$. Assume the initial values of model (2.3) $x(0) = x^* + x_{10},\ y(0) = y^* + y_{10}$ with $x_{10} = 1.35 \times 10^{-8}$, and $y_{10} = 1.35 \times 10^{-8}$. From Theorem 3.5, there is a resonance phenomenon of the solution $x(t)$ of model (2.3) when $\omega = \omega_{xr}$ (see Figure 4).

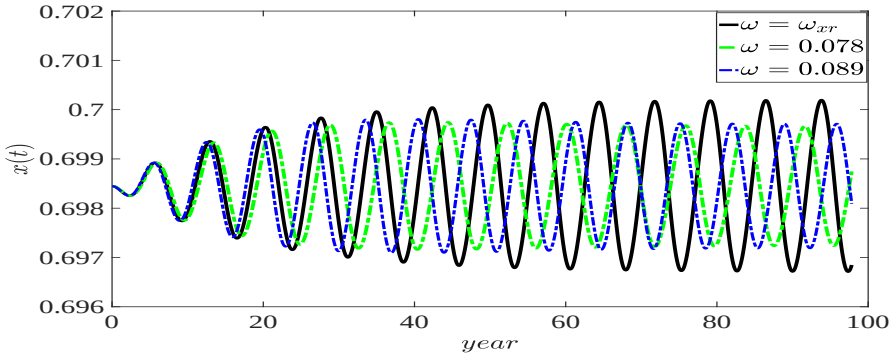

Figure 4. The solutions $x(t)$ of model (2.3) with $\omega = 0.078$, ω_{xr}, and 0.89.

These two resonance phenomena of $y(t)$ and $x(t)$ provide us with a new insight into the dynamics of model (2.3). The resonance phenomenon of the solution $y(t)$ of model (2.3) is our main concerned which provided a reasonable explanation for the concentrated outbreak of diseases and the potential threats it may cause, such as medical resource congestion.

To illustrate the attractivity of the resonance periodic solution $y(t)$ of model (2.3), we will present the following numerical examples.

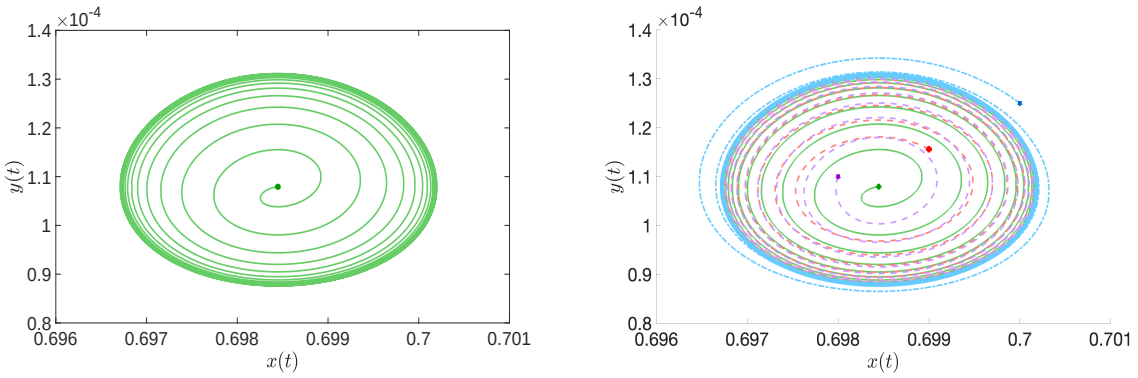

(a) The solution with $(x_0, y_0) = (0.698447, 0.000107919)$.

(b) Four solution curves.

Figure 5. The solution curves from different initial values tend to the resonance periodic trajectory if $\omega = \omega_r$.

From (4.1), (4.2), and Theorem 3.4, we know that the resonance of $y(t)$ occurs when $\omega = \omega_r$. Assume that the initial condition of model (2.3) is $(x(0), y(0)) = (0.698447, 0.000107919)$. Then, the phase diagram of model (2.3) is presented in Figure 5(a). After that, we choose four different initial conditions to numerically plot four solution curves (see Figure 5(b)), i.e., $(x(0), y(0)) = (0.698447, 0.000107919)$ (corresponding to the green line), $(x(0), y(0)) = (0.699, 0.0001156)$ (corresponding to the red line), $(x(0), y(0)) = (0.698, 0.00011)$ (corresponding to the purple line) and $(x(0), y(0)) = (0.7, 0.000125)$ (corresponding to the blue line). These results show that the resonance periodic solution $y(t)$ of model (2.3) may be attractive.

4.2. Data fitting and analysis

The parameters of model (2.3) are assumed as

$$\mu = 1.1 \times 10^{-3},\ \nu = 4.49,\ \eta = 3.402 \times 10^{-3},\ \omega = \frac{\pi}{5.49}. \tag{4.5}$$

The initial conditions are assumed to be $x(0) = \frac{1.1309\times10^9}{1.376\times10^9}$, $y(0) = \frac{18}{1.376\times10^9}$. From Figure 1, there is a periodic phenomenon of influenza in Shanghai from April 2014 to September 2016 [28]. Monthly reports of influenza incidence cases in Shanghai from April 2014 to September 2016 can be used to estimate the other parameters' values in model (2.3). Note that the time unit for reported new influenza cases is months. The incidence rate per unit of time of model (2.3) is denoted as D_i, i.e.,

$$D_i = \beta(1 + \Delta\beta \sin(\omega t_i))x(t_i)y(t_i)\ \ i = 1,\ 2,\ \cdots,\ 23.$$

Correspondingly, denote the number of the reported new influenza cases in the $i-$th month as X_i. In order to use the Markov chain Monte Carlo method (MCMC) to fit D_i to the new influenza cases X_i, we will multiply the reported new influenza cases X_i by multiplying $\frac{1}{1.376\times10^9}$ to balance the magnitudes.

Assume the initial values of the undetermined parameters $\Delta\eta_0$, $\Delta\beta_0$, β_0, and δ_0 are from the intervals $[0.11642, 0.11665]$, $[0.131618, 0.131621]$, $[5.52146, 5.52157]$, and $[0.015140, 0.015170]$, respectively. We use the MCMC method [33] to fit model (2.3) for $10,000$ iterations and get mean values, standard deviation values, and 95% confidence intervals (CI) of the unknown parameters $\Delta\eta$, $\Delta\beta$, β, and δ (see Table 1).

Table 1. Data fitting results for the parameters of model (2.3).

Parameter	Mean value	Std	95%CI	Resource
$\Delta\eta$	0.1171	0.002265095	$[0.1134, 0.1203]$	MCMC
$\Delta\beta$	0.1354	0.00370269	$[0.1305, 0.1428]$	MCMC
β	5.5081	0.0255497	$[5.4681, 5.5600]$	MCMC
δ	0.0150	0.00049715	$[0.0145, 0.0154]$	MCMC

From the 95% CI in Table 1, we choose

$$\begin{cases} \Delta\eta = 0.116542641395988, \quad \Delta\beta = 0.131620089096854, \\ \beta = 5.522128427495543, \quad \delta = 0.015155817773751. \end{cases} \tag{4.6}$$

Then, the model fit to the new influenza cases is shown in Figure 6.

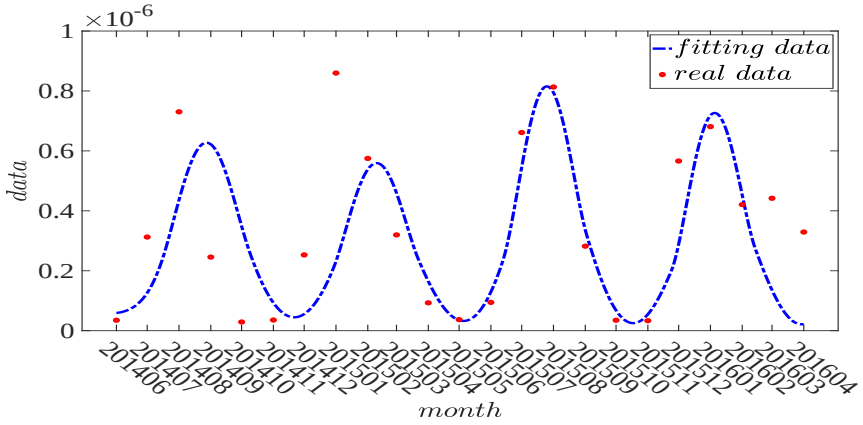

Figure 6. The fitted curve of the reported influenza data of model (2.3) with (4.6).

By use of (4.5) and (4.6), we calculate that $\mathcal{R}_{01} = 1.01678 > 1$, $\omega_{xr} = 0.035821093345414$, $s_r = 0.001449$, and $\omega_r = \sqrt{s_r} = 0.038075349047385$. Note that when $\omega = \frac{\pi}{5.49} \neq \omega_r \neq \omega_{xr}$, there is no resonance phenomenon of model (2.3), as follows from Theorems 3.4 and 3.5. To further reveal the effect of ω on the periodic solution of model (2.3), we choose

$$\omega = 0.0746, \ 0.18 \in \left(\omega_r, \ \frac{\pi}{5.49}\right).$$

Then, the solution $y(t)$ of model (2.3) can be plotted in Figure 7. These results show that the amplitude of the solution $y(t)$ is increasing as $\omega \to \omega_r^+$.

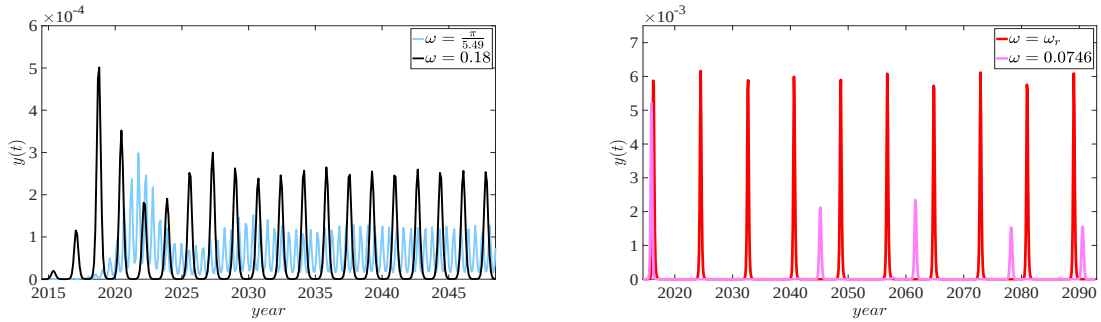

(a) $\omega = \frac{\pi}{5.49}$, $\omega = 0.18$. (b) $\omega = 0.0746$, $\omega = \omega_r$.

Figure 7. The influence of input frequency ω on the solution $y(t)$.

On the other hand, from the expression of the resonance frequency ω_r of (3.24), we find that the value of ω_r depends on the parameter δ. By use of (4.5) and (4.6), we plot the function of $\omega_r(\delta)$ (see Figure 8(b)). Numerical results show that the plot of $\omega_r = \omega_r(\delta)$ is a nonmonotonic curve, which intersects with the line $\omega = \frac{\pi}{5.49}$ at two points $\delta_1^* = 0.35624$ and $\delta_2^* = 1.65069$. From Theorem 3.4, the resonance phenomenon of model (2.3) will occur when $\delta = \delta_i^*$ $(i = 1, 2)$. Meanwhile, we can treat ω_r as a function of β from the expression of (3.24). Under condition (4.5), we can plot the function $\omega_r(\beta)$ (see Figure 8(a)). Numerical results show that the plot of $\omega_r(\beta)$ intersects with the line $\omega = \frac{\pi}{5.49}$ at a unique point $\beta^* = 1.03783 \times 10^{-6}$. From Theorem 3.4, the resonance phenomenon of model (2.3) will occur when $\beta = \beta^*$.

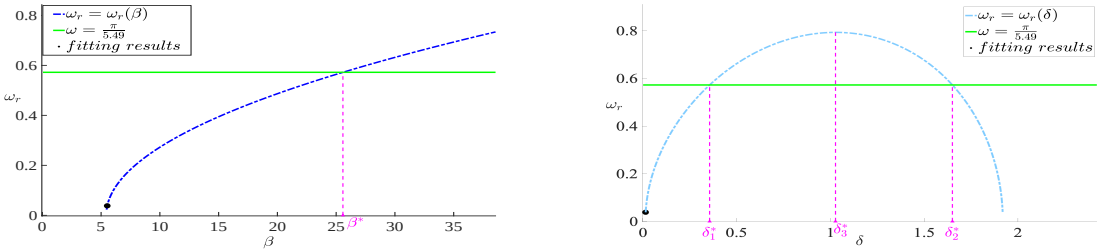

(a) The plot of $\omega_r(\beta)$ for $\beta \in (0, 1.4 \times 10^{-6})$. (b) The plot of $\omega_r(\delta)$ for $\delta \in (0, 2.5)$.

Figure 8. The dependence of the resonant frequency ω_r on the parameter δ, β.

Figure 8(b) shows that the value of the resonance frequency $\omega_r(\delta)$ is non-monotonic and has a maximum point δ_3^*. The resonance frequency $\omega_r(\delta)$ increases for $\delta \in (0, \delta_3^*)$ and then decreases for $\delta > \delta_3^*$. From (3.21), the amplitude of $y_1(t)$ is determined by $g(\omega)$, we calculate the value of $g(\omega_r(\delta))$ when $\delta = \delta_1,\ \delta_2, \delta_1^*,\ \delta_3,\ \delta_4,\ \delta_5,\ \delta_6,\ \delta_2^*,\ \delta_7,\ \delta_8$ and the results are presented in Table 2. By use of (4.5), (4.6), and Table 2, the solutions $y(t)$ of model (2.3) are plotted when $\omega = \omega_r(\delta)$ and $\delta = \delta_1,\ \delta_2,\ \delta_1^*,\ \delta_3,\ \delta_4,\ \delta_5,\ \delta_6,\ \delta_2^*,\ \delta_7,\ \delta_8$, respectively (see Figure 9). Calculation and numerical results show that the period $\frac{2\pi}{\omega_r}$ of $y(t)$ of model (2.3) decreases for $\delta \in (0, \delta_3^*)$ and then increases for $\delta > \delta_3^*$, while the amplitude of $y(t)$ when $\omega = \omega_r(\delta)$ increases strictly monotonically as the value of δ increases (see Figure 9).

Table 2. The calculation results of $g(\omega)$ and ω_r.

Parameter	δ_1	δ_2	δ_1^*	δ_3	δ_4	δ_5	δ_6	δ_2^*	δ_7	δ_8
δ	0.15	0.25	0.3562	0.45	0.55	1.35	1.45	1.6506	1.75	1.85
$\omega_r(\delta)$	0.371	0.483	$\frac{\pi}{5.49}$	0.633	0.686	0.741	0.701	$\frac{\pi}{5.49}$	0.470	0.311
$g(\omega_r)\cdot 10^{-2}$	0.172	0.705	1.046	1.096	1.133	2.426	2.682	3.250	3.558	3.886

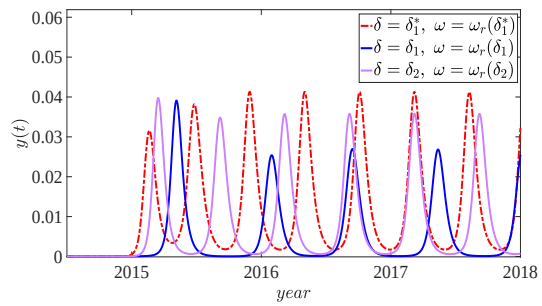

(a) $\delta=\delta_1,\ \delta_2,\ \delta_1^*,\ \omega=\omega_r(\delta_1),\ \omega_r(\delta_2),\ \omega_r(\delta_1^*)$.

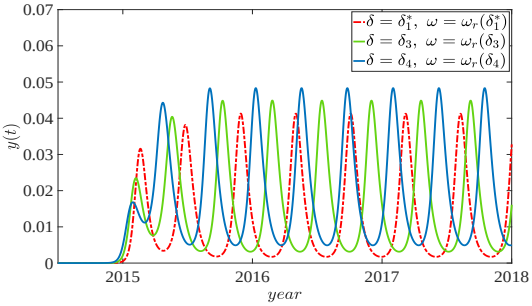

(b) $\delta=\delta_1^*,\ \delta_3,\ \delta_4,\ \omega=\omega_r(\delta_1^*),\ \omega_r(\delta_3),\ \omega_r(\delta_4)$.

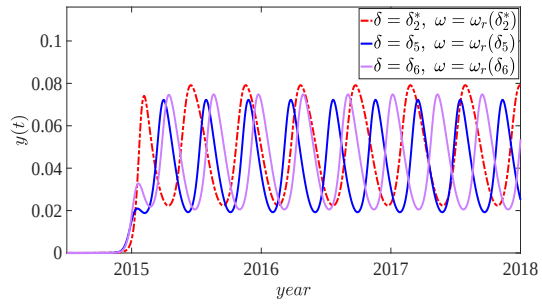

(c) $\delta=\delta_5,\ \delta_6,\ \delta_2^*,\ \omega=\omega_r(\delta_5),\ \omega_r(\delta_6),\ \omega_r(\delta_2^*)$.

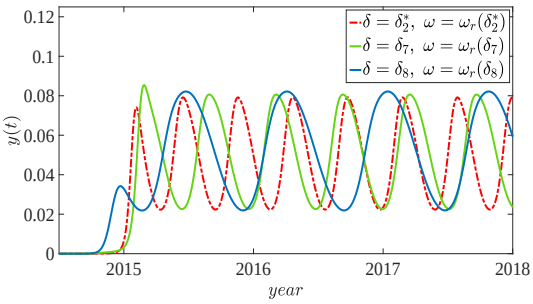

(d) $\delta=\delta_2^*,\ \delta_7,\ \delta_8,\ \omega=\omega_r(\delta_2^*),\ \omega_r(\delta_7),\ \omega_r(\delta_8)$.

Figure 9. The influence of δ on the solution $y(t)$ when resonance occurs.

Figure 8(a) shows that the value of the resonance frequency $\omega_r(\beta)$ is monotonically increasing for $\beta > 0$. From (3.21), the amplitude of $y_1(t)$ is determined by $g(\omega)$, we calculate the value of $g(\omega_r(\beta))$ when $\beta = \beta_1,\ \beta_2, \beta^*,\ \beta_3,\ \beta_4$, and the results are presented in Table 3. By use of (4.5), (4.6), and Table 3, the solutions $y(t)$ of model (2.3) are plotted when $\omega = \omega_r(\beta)$ and $\beta = \beta_1,\ \beta_2, \beta^*,\ \beta_3,\ \beta_4$, respectively (see Figure 10). Calculation and numerical results show that the period $\frac{2\pi}{\omega_r}$ of $y(t)$ of model (2.3) is monotonically decreasing when $\beta > 0$, while the amplitude of $y(t)$ when $\omega = \omega_r(\beta)$ is non-monotonic and has a maximum point β^* (see Figure 9).

Table 3. The calculation results of $g(\omega)$ and ω_r.

Parameter	β_1	β_2	β^*	β_3	β_4
β	19.714	22.179	25.575	49.286	79.929
$\omega_r(\beta)$	0.48186	0.52177	$\frac{\pi}{5.49}$	0.84433	1.05522
$g(\omega_r)$	0.00148	0.00335	0.00673	1.50762×10^{-4}	4.05188×10^{-5}

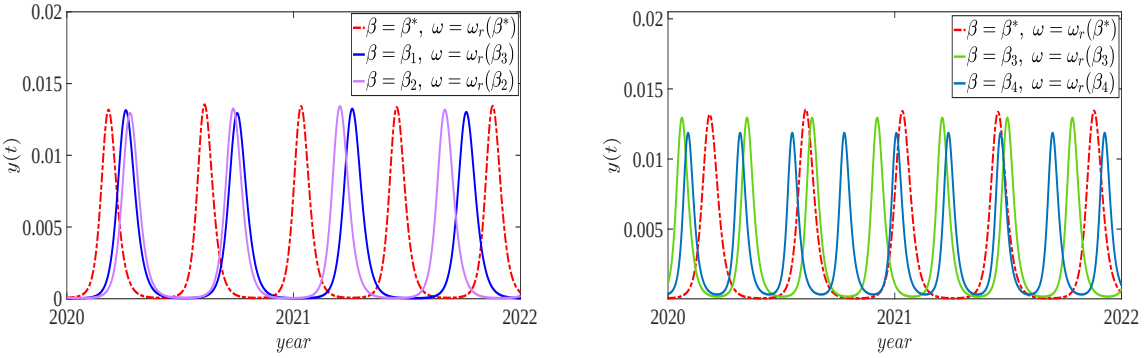

(a) $\beta = \beta_1, \beta_2, \beta^*, \omega = \omega_r(\beta_1), \omega_r(\beta_2), \omega_r(\beta^*)$. (b) $\beta = \beta^*, \beta_3, \beta_4, \omega = \omega_r(\beta^*), \omega_r(\beta_3), \omega_r(\beta_4)$.

Figure 10. The solutions $y(t)$ for model (2.3) when resonance phenomena occur.

To illustrate the effect of the periodic vaccination, we assume $\Delta\eta = 0$ (i.e., there is a constant vaccination rate), and then get the the resonance frequency ω_{0r}. By use of (4.5) and (4.6), the plots of ω_{0r} and ω_r with respect to δ are presented in Figure 11(a), which shows that the constant vaccination rate also results in resonance phenomena.

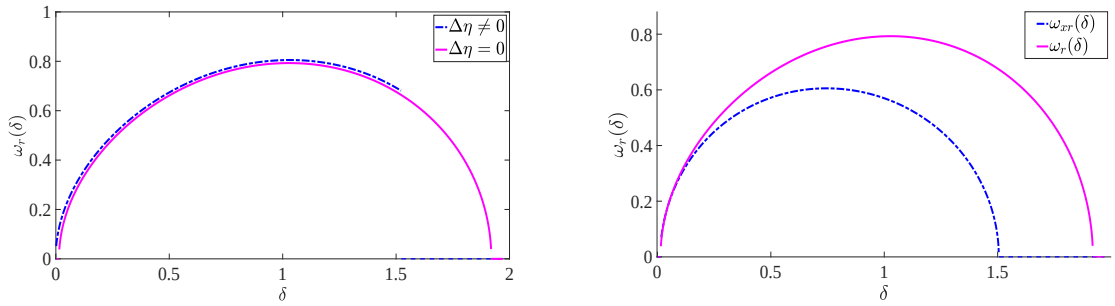

(a) $\Delta\eta = 0$ and $\Delta\eta \neq 0$. (b) The graphs of $\omega_r(\delta)$ and $\omega_{xr}(\delta)$.

Figure 11. The influence of δ and $\Delta\eta$ on the resonance frequencies.

Note that the resonance frequencies of $y(t)$ and $x(t)$ of model (2.3) are ω_r and ω_{xr}, respectively. By use of (4.5) and (4.6), the plots of ω_r and ω_{xr} with respect to δ are presented in Figure 11(b). These results show that the values of ω_r and ω_{xr} are very close when δ is sufficiently small. As the value of δ increases, the difference between ω_r and ω_{xr} becomes larger and larger. The transition rate from the recovered to the susceptible, δ, reflects the short period of immunity of the recovered and can also influence the magnitude of the difference between the two frequencies ω_r and ω_{xr}. The longer the immune period of the recovered is, the more likely it is to cause the simultaneous resonance phenomenon of $x(t)$ and $y(t)$. Inversely, the shorter the immune period of the recovered is, the less likely it is to cause the simultaneous resonance phenomenon of $x(t)$ and $y(t)$.

5. Conclusions and discussion

In this paper, we proposed an $SIRS$ epidemic model with periodic transmission rate $\beta(t)$ and periodic vaccination rate $\eta(t)$ to model the periodic spread dynamics of the influenza. In the modeling and the process of the dynamic analysis of our model, the common factor of transmission frequency and vaccination frequency, ω, played an important role. The elementary dynamic results of our model are proved, i.e., the disease-free periodic steady state of model (2.3) is globally asymptotically stable when the basic reproduction number $\mathcal{R}_0 < 1$, and model (2.3) is uniformly persistent when the basic reproduction number $\mathcal{R}_0 > 1$. After that, with the help of the resonance theory, we found that there are resonance phenomena of $y(t)$ and $x(t)$ of model (2.3) when $\omega = \omega_r$ and $\omega = \omega_{xr}$, respectively (see Theorems 3.4 and 3.5). Some numerical simulations were carried out to illustrate the resonance phenomena.

In addition, by use of the monthly infected cases of influenza in Shanghai from June 2014 to April 2016, we fitted the parameters of our epidemic model (2.3) (see Table 1 for the fitted results). By use of the results in Table 1, we calculated that if $\omega \neq \omega_r$ and $\omega \neq \omega_{xr}$, then there are no resonance phenomena of $y(t)$ and $x(t)$ in our epidemic model (2.3), as follows from Theorems 3.4 and 3.5. However, a resonance phenomenon of $y(t)$ in model (2.3) will occur as the value of the mean transmission rate β increases (i.e., when $\beta = \beta^*$), which is verified by some numerical simulations in Section 4.2. Besides that, a resonance phenomenon of $y(t)$ of model (2.3) will also occur as the value of transition rate δ changes (i.e., when $\delta = \delta_1^*$ or $\delta = \delta_2^*$), which is also verified by some numerical simulations in Section 4.2.

In the existing $SIRS$ disease models, stable positive periodic solution phenomena often occur. Some of these are caused by short-term immunity or immune delay, resulting in Hopf bifurcations in autonomous $SIRS$ models; others are the existence of positive periodic steady-states in non-autonomous periodic $SIRS$ models. All of the above can be rigorously proved by use of mathematical theories. In this paper, the existence of the resonant periodic solution of the periodic epidemic model (2.3) studied by use of the resonance theory, which is a special type of solution of model (2.3) induced by the input frequency ω. It mainly focuses on studying the influence of the input frequency on the amplitude of the periodic solution. Due to the lack of mathematical theoretical tools, the attractivity and stability of this resonant periodic solution are not proved. Some numerical examples are used to illustrate the attractivity of the resonant periodic solutions (see Figure 5).

The research content of this paper provides a theoretical basis for avoiding the occurrence of resonance periodic solutions and preventing medical congestion phenomena, and offers a new perspective for us to understand the periodic transmission of influenza diseases. The methods used in this paper can be used to study the spread of other periodic infectious diseases.

Use of AI tools declaration

The authors declare they have not used Artificial Intelligence (AI) tools in the creation of this article.

Acknowledgments

This work is supported by the National Natural Science Foundation of China No. 12271143.

Conflict of interest

Professor Xichao Duan is a Guest Editor of special issue "Population ecology and the dynamic modeling of epidemics" for Electronic Research Archive. He was not involved in the editorial review and the decision to publish this article. The authors declare there are no conflicts of interest.

References

1. K. G. Nicholson, R. G. Webster, A. J. Hay, Textbook of Influenza, *Trans. R. Soc. Trop. Med. Hyg.*, **93** (1999), 31. https://doi.org/10.1016/S0035-9203(99)90169-4
2. J. N. Barr, R. Fearns, Chapter 2 - Genetic instability of RNA viruses, *Genome Stab.*, (2016), 21–35. https://doi.org/10.1016/B978-0-12-803309-8.00002-1
3. S. Cauchemez, A. Valleron, P. Boëlle, A. Flahault, N. M. Ferguson, Estimating the impact of school closure on influenza transmission from Sentinel data, *Nature*, **452** (2008), 750–754. https://doi.org/10.1038/nature06732
4. L. Shi, L. Wang, Z. Jin, The seasonal influenza transmission dynamic and the correlation analysis with meteorology in Beijing, *Int. J. Biomath.*, **17** (2024), 2350071. https://doi.org/10.1142/S1793524523500717
5. J. Shaman, E. Goldstein, M. Lipsitch, Absolute humidity and pandemic versus epidemic influenza, *Am. J. Epidemiol.*, **173** (2011), 127–135. https://doi.org/10.1093/aje/kwq347
6. G. Neumann, Y. Kawaoka, Seasonality of influenza and other respiratory viruses, *EMBO Mol. Med.*, **14** (2022), e15352. https://doi.org/10.15252/emmm.202115352
7. Y. L. Shu, W. Liu, S. Vlas, Y. Gao, J. H. Richardus, W. C. Cao, Dual seasonal patterns for influenza, China, *Emerging Infect. Dis.*, **16** (2010), 725–726. https://doi.org/10.3201/eid1604.091578
8. Y. Z. Zhang, C. C. Ye, J. X. Yu, W. P. Zhu, Y. P. Wang, Z. J. Li, et al., The complex associations of climate variability with seasonal influenza A and B virus transmission in subtropical Shanghai, China, *Sci. Total Environ.*, **701** (2020), 134607. https://doi.org/10.1016/j.scitotenv.2019.134607
9. J. L. Ma, J. Dushoff, D. Earn, Age-specific mortality risk from pandemic influenza, *J. Theor. Biol.*, **288** (2011), 29–34. https://doi.org/10.1016/j.jtbi.2011.08.003
10. J. Arino, C. Bauch, F. Brauer, S. M. Driedger, A. L. Greer, S. M. Moghadas, et al., Pandemic influenza: Modelling and public health perspectives, *Math. Biosci. Eng.*, **8** (2011), 1–20. https://doi.org/10.3934/mbe.2011.8.1
11. S. M. Asaduzzaman, J. L. Ma, P. Driessche, Estimation of cross-immunity between drifted strains of influenza A/H3N2, *Bull. Math. Biol.*, **80** (2018), 657–669. https://doi.org/10.1007/s11538-018-0395-5
12. D. H. He, J. Dushoff, T. Day, J. L. Ma, D. Earn, Mechanistic modelling of the three waves of the 1918 influenza pandemic, *Theor. Ecol.*, **4** (2011), 283–288. https://doi.org/10.1007/s12080-011-0123-3
13. S. M. Asaduzzaman, J. L. Ma, P. Driessche, The coexistence or replacement of two subtypes of influenza, *Math. Biosci.*, **270** (2015), 1–9. https://doi.org/10.1016/j.mbs.2015.09.006

14. Y. Furuse, H. Oshitani, Mechanisms of replacement of circulating viruses by seasonal and pandemic influenza A viruses, *Int. J. Infect. Dis.*, **51** (2016), 6–14. https://doi.org/10.1016/j.ijid.2016.08.012

15. Z. McCarthy, S. Athar, M. Alavinejad, C. Chow, I. Moyles, K. Nah, et al., Quantifying the annual incidence and underestimation of seasonal influenza: a modelling approach, *Theor. Biol. Med. Modell.*, **17** (2020), 11. https://doi.org/10.1186/s12976-020-00129-4

16. X. C. Duan, J. F. Yin, X. Z. Li, Global Hopf bifurcation of an SIRS epidemic model with age-dependent recovery, *Chaos, Solitons Fractals*, **104** (2017), 613–624. https://doi.org/10.1016/j.chaos.2017.09.029

17. T. L. Zhang, J. L. Liu, Z. D. Teng, Stability of Hopf bifurcation of a delayed SIRS epidemic model with stage structure, *Nonlinear Anal. Real World Appl.*, **11** (2010), 293–306. https://doi.org/10.1016/j.nonrwa.2008.10.059

18. H. Cao, X. Y. Gao, J. Q. Li, D. X. Yan, Z. M. Yue, The bifurcation analysis of an SIRS epidemic model with immunity age and constant treatment, *Appl. Anal.*, **100** (2021), 2844–2866. https://doi.org/10.1080/00036811.2019.1698728

19. S. Gakkhar, K. Negi, Pulse vaccination in SIRS epidemic model with non-monotonic incidence rate, *Chaos, Solitons Fractals*, **35** (2008), 626–638. https://doi.org/10.1016/j.chaos.2006.05.054

20. S. L. Jing, H. F. Huo, H. Xiang, Modelling the effects of ozone concentration and pulse vaccination on seasonal influenza outbreaks in Gansu province, China, *Discrete Contin. Dyn. Syst. - Ser. B*, **27** (2022), 1877–1911. https://doi.org/10.3934/dcdsb.2021113

21. Z. D. Teng, Y. P. Liu, L. Zhang, Persistence and extinction of disease in non-autonomous SIRS epidemic models with disease-induced mortality, *Nonlinear Anal. Theory Methods Appl.*, **69** (2008), 2599–2614. https://doi.org/10.1016/j.na.2007.08.036

22. B. Chaihao, S. Khomrutai, Extinction and permanence of a general non-autonomous discrete-time SIRS epidemic model, *AIMS Math.*, **8** (2023), 9624–9646. https://doi.org/10.3934/math.2023486

23. A. Kumar, N. Kumari, S. Manda, P. K. Tiwari, Autonomous and non-autonomous dynamics of an SIRS model with convex incidence rate, *J. Franklin Inst.*, **362** (2025), 108236. https://doi.org/10.1016/j.jfranklin.2025.108236

24. W. C. Zhao, J. L. Liu, M. N. Chi, F. F. Bian, Dynamics analysis of stochastic epidemic models with standard incidence, *Adv. Differ. Equations*, **2019** (2019), 22. https://doi.org/10.1186/s13662-019-1972-0

25. I. A. Moneim, Modeling and simulation of the spread of H1N1 flu with periodic vaccination, *Int. J. Biomath.*, **9** (2016), 1650003. https://doi.org/10.1142/S1793524516500030

26. J. Dushoff, J. B. Plotkin, S. Levin, D. Earn, Dynamical resonance can account for seasonality of influenza epidemics, *Proc. Natl. Acad. Sci. U.S.A.*, **101** (2004), 16915–16916. https://doi.org/10.1073/pnas.0407293101

27. G. F. Franklin, J. D. Powell, A. Emami-Naeini, *Feedback Control of Dynamic Systems*, Pearson, 2019.

28. Shanghai Municipal Health Commission, Report on the Epidemic Situation of Legally notifiable Infectious Diseases in Shanghai. Available from: https://wsjkw.sh.gov.cn/yqxx/index.html.

29. N. Bacaër, S. Guernaoui, The epidemic threshold of vector-borne diseases with seasonality, *J. Math. Biol.*, **53** (2006), 421–436. https://doi.org/10.1007/s00285-006-0015-0
30. W. Wang, X. Q. Zhao, Threshold dynamics for compartmental epidemic models in periodic environments, *J. Dyn. Differ. Equations*, **20** (2008), 699–717. https://doi.org/10.1007/s10884-008-9111-8
31. X. Q. Zhao, *Dynamical Systems in Population Biology*, Springer International Publishing, 2017. https://doi.org/10.1007/978-3-319-56433-3
32. H. R. Thieme, Persistence under relaxed point-dissipativity (with application to an endemic model), *SIAM J. Math. Anal.*, **24** (1993), 407–435. https://doi.org/10.1137/0524026
33. H. Haario, M. Laine, A. Mira, E. Saksman, Dram: efficient adaptive MCMC, *Stat. Comput.*, **16** (2006), 339–354. https://doi.org/10.1007/s11222-006-9438-0

Appendix

A. Proof of Theorem 3.2.

Proof. Note that the unique solution of model (2.3) starting from $\mathbb{R}^2_+$ exists for all $t > 0$ and remains non-negative. For such a solution, we have

$$\frac{dx(t)}{dt} \leq (\mu + \delta) - (\mu + \delta + \eta(t))x(t).$$

By the comparison principle and (3.4), we have

$$x(t) < x^0(t) + \epsilon, \text{ for large enough } t, \tag{A.1}$$

where $\epsilon > 0$ is given, and $x^0(t)$ is the solution of (3.4). It follows from (*A*.1) and the second equation of model (2.3) that

$$\frac{dy(t)}{dt} < \beta(t)(x^0(t) + \epsilon)y(t) - (\mu + \nu)y(t).$$

Then, we have

$$y(t) < \tilde{y}(t), \tag{A.2}$$

where the auxiliary variable $\tilde{y}(t)$ satisfies the following equation

$$\begin{cases} \dfrac{d\tilde{y}(t)}{dt} = \beta(t)(x^0(t) + \epsilon)\tilde{y}(t) - (\mu + \nu)\tilde{y}(t), \\ \tilde{y}(0) = y_0. \end{cases} \tag{A.3}$$

Let $\mathcal{F}(\epsilon)(t) = \beta(t)(x^0(t) + \epsilon)$. Then, we define the perturbation of the next generation operator $\mathcal{L}$ as follows:

$$\mathcal{L}(\epsilon)(\phi(t)) = \int_0^\infty \mathcal{Y}(t, t-a)\mathcal{F}(\epsilon)(t-a)\phi(t-a)da.$$

The spectral radius of $\mathcal{L}(\epsilon)$ is denoted as $\mathcal{R}_0(\epsilon)$. Note that the operator $\mathcal{L}$ is continuous with respect to ϵ. It follows that $\mathcal{R}_0(\epsilon) \to \mathcal{R}_0$ as $\epsilon \to 0$. If $\mathcal{R}_0 < 1$, there exists an $\epsilon > 0$ which is small enough such that $\mathcal{R}_0(\epsilon) < 1$. By Theorem 2.2 in [30], we can obtain $\tilde{y}(t) \to 0$ as $t \to \infty$. Therefore, it follows from (*A*.2) that the solution of model (2.3) satisfies $y(t) \to 0$ as $t \to \infty$, then we obtain $x(t) \to x^0(t)$ as $t \to \infty$. Therefore, the disease-free periodic equilibrium E^0 of model (2.3) is globally asymptotically stable.

B. Proof of Theorem 3.3.

Proof. Let $Q(t) = x(t) + y(t)$. By direct calculations, we have

$$\begin{aligned}\frac{dQ(t)}{dt} =&(\mu + \delta) - (\mu + \delta)(x(t) + y(t)) - \eta(t)x(t) - \nu y(t)\\ \leq&(\mu + \delta) - (\mu + \delta)Q(t).\end{aligned}$$

Thus, $Q(t) < 1$ for all large time t. As a result, the set $\{(x, y) \in \mathbb{R}^2_+ : Q = x + y < 1\}$ is a positively invariant set of model (2.3). It is not difficult to determine that H_0 is positively invariant.

It is clear that $\{(x^0(t), 0)\}$ is the omega limit set of model (2.3) in ∂H_0, i.e., the solution of model (2.3) starting from ∂H_0 reaches E^0 as t goes to infinity. So, ∂H_0 is the positive invariant set of model (2.3).

Let $\varphi(t, X_0)$ be the solution of model (2.3) with $\varphi(0, X_0) = X_0 = (x(0), y(0))^T$, and P be the *Poincaré* map induced by model (2.3), that is, $P(X_0) = \varphi(T_0, X_0)$. T_0 is the period of the solution of model (2.3). By [31], the uniform persistence of model (2.3) is equivalent to that of the discrete semi-dynamical system $\{P^n\} := \mathcal{D}$.

We show below that E^0 repels weakly the positive orbits of $\mathcal{D}$ with $(x(0), y(0))^T \in H_0$. By contradiction, we suppose that for $\forall \epsilon > 0$, there is a positive solution $(x(t), y(t))$ of model (2.3) with $(x(0), y(0))^T \in H_0$ such that

$$\left|x(nT_0) - x^0(0)\right| < \epsilon, \quad |y(nT_0) - 0| < \epsilon.$$

Then there exists a positive constant M, such that

$$\left|x(t) - x^0(t)\right| < \epsilon, \quad |y(t)| < \epsilon, \tag{B.1}$$

for $n > M$ and $\forall\ t \geq nT_0$, i.e.,

$$x^0(t) - \epsilon < x(t) < x^0(t) + \epsilon. \tag{B.2}$$

Substituting $(B.2)$ into the second equation of model (2.3), we obtain

$$\frac{dy(t)}{dt} > \beta(t)(x^0(t) - \epsilon)y(t) - (\mu + \nu)y(t).$$

Then, we have

$$y(t) > \hat{y}(t), \tag{B.3}$$

where the auxiliary variable $\hat{y}(t)$ satisfies

$$\begin{cases}\dfrac{d\hat{y}(t)}{dt} = \beta(t)(x^0(t) - \epsilon)\hat{y}(t) - (\mu + \nu)\hat{y}(t),\\ \hat{y}(0) = y_0.\end{cases} \tag{B.4}$$

Let $\mathcal{F}(-\epsilon)(t) = \beta(t)(x^0(t) - \epsilon)$, a relatively systematic next generation operator is defined by

$$\mathcal{L}(-\epsilon)\phi(t) = \int_0^\infty \mathcal{Y}(t, t - a)\mathcal{F}(-\epsilon)(t - a)\phi(t - a)da.$$

Denote $\mathcal{R}_0(-\epsilon)$ as the spectral radius of $\mathcal{L}(-\epsilon)$. Notice that the operator $\mathcal{L}$ is continuous. If $\mathcal{R}_0 > 1$, there exists an $\epsilon > 0$ small enough such that $\mathcal{R}_0(-\epsilon) > 1$. Therefore, by [31] and Theorem 2.2 in [30],

the solution of $(B.4)$ satisfies $\hat{y}(t) \to \infty$ as $t \to \infty$. By the comparison principle and $(B.3)$, the solution of model (2.3) satisfies $y(t) \to \infty$ as $t \to \infty$, which contradicts with the boundedness of H_0. Therefore, the disease-free periodic equilibrium E^0 repels weakly the positive H_0, and the disease described by model (2.3) is uniformly persistent with respect to $(H_0, \partial H_0)$.

AIMS Press